Safety of Stereo Driver Assistance Systems

Waqar Khan, John Morris

The University of Auckland, New Zealand
wkha011@aucklanduni.ac.nz, j.morris@auckland.ac.nz

Abstract. The discrete nature of disparities observed by stereo systems results in complex behaviour of speeds measured by them and affects the efficacy of a stereo based driver assistance system. We describe a tool for a safety engineer which permits the safety of these systems to be estimated. It is based on a model which considers the true error in measured velocities of objects. Outputs from this tool show that choice of stereo system parameters so as to judiciously place the disparity change boundaries is critical to the effectiveness of such a system because the range of possible trajectories for a (possibly colliding) object reduces significantly when a feature point on that object crosses one of these boundaries. This factor also means that larger objects (*e.g.* trucks) are slightly better tracked by stereo than smaller ones (*e.g.* signs and pedestrians). Completely safe stereo based systems are also shown to issue many precautionary (and ultimately unnecessary) warnings if the stereo parameters are not chosen carefully.

1 Introduction

Numerous algorithms have been proposed for deriving disparity maps from stereo pairs[1]. However, there have been relatively few studies of the depth accuracy of stereo. Stereo is being actively studied for safety systems, so determining its accuracy is crucial[2,3,4]. There are several sources of measurement inaccuracy:

- Disparity values are usually integral, therefore measured depths are quantized [5]. Some stereo algorithms generate disparities with sub-pixel accuracy, but the output still corresponds to a discrete set.
- System latency means that depth values are not available until a significant time after the images were captured: this ranges from, at best, a few scanlines[6], to one or more full frame times[7].
- Accuracy in stereo matching algorithms is directly related to the hardware requirements. Scan line based algorithms are fast and have less hardware needs as compared to more accurate global correspondence algorithms like belief propagation [8].

Depth accuracy depends upon an object's location within the stereo Common Field of View (CFoV) - the region imaged onto *both* cameras from which depth information can be obtained. A stereo based system's estimate of an opposing object's velocity becomes significantly more accurate over a few time samples (frames) since it was first observed [9]. In a safety system, the time taken to accurately estimate the trajectory of a potential danger is clearly vital. The earlier the system knows the correct trajectory, the earlier it can generate a warning or avoid a hazard. Early warnings increase confidence in the system [10,11]. Conversely, late warnings lead to a loss in confidence in the system. Therefore a system must generate a timely and accurate warning.

A stereo system designer works in a wide design space considering the optical characteristics of the system - lenses, baseline, image resolution, etc - as well as vehicle handling parameters - speed, braking distance and turning ability. To aid a safety engineer to determine the efficacy of a stereo based safety system, our model shows how fast potential hazards can move and still be effectively detected and avoided by the system. Our model assumes that a hazard can 'appear from nowhere', *i.e.* pedestrians walk out from behind parked cars or vehicles appear from behind other vehicles: so an object may first be observed at any position. It shows a safety engineer how changing optical and vehicle parameters effect the stereo component of a safety system. Effectiveness is measured by the highest speed that an opposing object (other car, pedestrian or static hazard) can have and still be safely detected. 'Safely detected' means that the object's trajectory is correctly predicted in time to brake. Our model outputs a contour map showing the maximum 'safe' speed for objects in the vicinity of our vehicle. This single map gives an overall view of the ability of the stereo system to warn the driver in time to avoid or mitigate hazards and highlights limitations of the stereo component. The system must ensure that the impacts occur at less than some threshold speed - to avoid either death or serious injury to the colliding pedestrian or driver. We assume that low speed collisions in which no one is injured, whilst undesirable, are 'safe' and add a maximum tolerable collision speed, V^i_{crit}, to the model. V^i_{crit} varies with scenarios and the amount of protection necessary for road users[12] (see Figure 1). We assume that low speed collisions in which no one is injured, whilst undesirable, are 'safe' and add a maximum tolerable collision speed, V^i_{crit}, to the model.

The model consists of a series of constraints each of which can further reduce the speed of an opposing object that the system can handle. Clearly, the first constraint is 'unavoidable collision' - an object is traveling so fast that the system cannot take any action to avoid a collision: this sets an upper limit to the speed for which our system is useful. Note that even if a collision is inevitable, a timely warning can mitigate damage by braking or turning to avoid the opposing object.

Here, we assume that the only collision avoidance strategy is braking[1]. Thus the deceleration generated by the brakes is a key parameter in our safety model.

[1] We exclude turning because it is not always a safe avoidance strategy, *e.g.* when driving is constrained by highway lanes. Future work should consider adaptive strategies and include additional vehicle characteristics, such as angular acceleration.

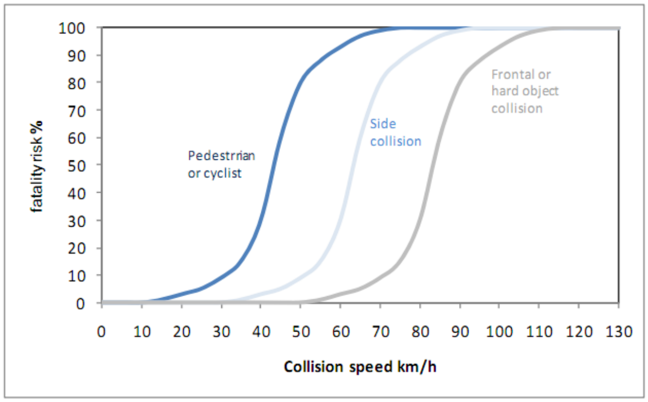

Fig. 1. Collision speed V^i_{crit}: V^i_{crit} varies with scenarios and the amount of protection needed for the road users[12].

2 Model

2.1 Colliding object

Assume a rigid object of size $L \times H \times W$ traveling at constant velocity, $\overrightarrow{V} = [V_x, V_y, V_z]^T$, in the same direction as its L dimension, first appears at $\overrightarrow{O(0)} = [O_x(0), O_y(0), O_z(0)]^T$. The reference point for the object will usually be the point closest to our vehicle.

2.2 Our vehicle

Our vehicle - initially at $\overrightarrow{O^i(0)} = \left[O^i_x(0), O^i_y(0), O^i_z(0)\right]^T$ - also travels at constant velocity, $\overrightarrow{V^i}$ along the Z axis so that $O^i_x = V^i_x = 0$. We place an exclusion zone of radius, r_{exc}, around our vehicle and set it slightly larger than a typical vehicle to allow for the psychological impact of a near miss on a driver's confidence - too many near misses and the system will certainly not be trusted!
Our model is currently restricted to vehicles and objects moving on a flat surface, so we set all y-components to 0.

2.3 Model basics

We can derive:

- Object's position at time, t, $\overrightarrow{O(t)} = \overrightarrow{O(0)} + \overrightarrow{V}t$
- The object's trajectory angle, $\eta = tan^{-1}\left(\frac{V_z}{V_x}\right)$ relative to the X-axis
- It 'enters' our path ($i.e.$ crosses the $X = r_{exc}$) at time,

$$t_{cross} = \frac{-O_x(0) + r_{exc} - W\sin\eta}{V_x} \tag{1}$$

at position, $\overrightarrow{O(t_{cross})} = [r_{exc}, 0, Z_{cross}]^T$, where $Z_{cross} = O_z(0) - V_z t_{cross}$

– and 'leaves' it after

$$t_{leave} = \frac{-O_x(0) - r_{exc} + L\cos\eta}{V_x} \tag{2}$$

at $Z_{leave} = O_z(0) - V_z t_{leave}$

– At t_{cross}, our vehicle's exclusion zone is centred on $\overrightarrow{O^i(t_{cross})} = \overrightarrow{O^i(0)} + V^i t_{cross}$
– We will have a collision if the separation between the object and our vehicle, $D_c = \sqrt{(O_x(t) - O_x^i(t))^2 + (O_z(t) - O_z^i(t))^2} \le r_{exc}$.
– If the system can generate a warning before $t_{warn} = t_{cross} - t_b - t_d$, when our vehicle is at $[0, 0, Z_{cross} - D_b]^T$ (see Section 2.4), then our vehicle will slow to less than V_{crit}^i in time.

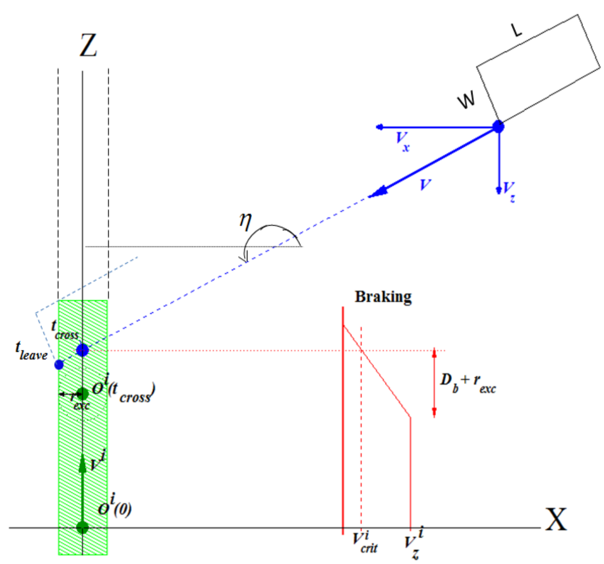

Fig. 2. Collision scenario

2.4 Design Constraints

The stereo system works in a relative frame centred on our vehicle: a superscript r denotes quantities in this frame, so $\overrightarrow{O^r(t)} = \overrightarrow{O(t)} - \overrightarrow{O^i(t)}$ and collision angle $\zeta = tan^{-1}(\frac{-O_z^r(t)}{-O_x^r(t)})$. The stereo system and our vehicle's capabilities introduce the following constraints:

Extent of the stereo CFoV We assume that the safety system has two cameras, each with $w \times h$ square pixels of size, τ, in a canonical stereo configuration, with baseline, b, focal length, f, and vergence angle, $\phi = 0$.
The angular extent of the CFoV is 2θ where

$$\theta = tan^{-1}(\frac{w\tau}{2f}) \tag{3}$$

The maximum disparity that the stereo system can process, d_{max}, determines the closest distance at which depth can be measured: $Z_{min} = \frac{fb}{d_{max}}$. A point at $\overrightarrow{O^r(t)}$ is observable in the stereo CFoV if $-\theta \leq tan^{-1}\left(\frac{O^r_x(t)}{O^r_z(t) - b/(2\tan\theta)}\right) \leq \theta$ and its distance may be measured if $O^r_z(t) \geq Z_{min}$.
We consider, n equidistant feature points over the object's extent. So, for each feature point this constraint is applicable.

Depth resolution For a feature point at $(u_{L|R}, v)$ relative to the principal point on the image plane of the left|right camera, the disparity, $d = u_L - u_R$. The depth resolution (or smallest change in distance that can be measured), $\delta Z(d)$, increases with distance. The depth resolution at disparity, d, is the difference between the depth corresponding to sequential disparity values, d and $d + 1$:

$$\delta Z(d) = \frac{fb}{\tau}(\frac{1}{d} - \frac{1}{d+1}) \tag{4}$$

and the uncertainty in depth for a feature point appearing to be at depth $\widehat{Z}^r$ is

$$\varDelta Z(d) = \frac{\delta Z(d) + \delta Z(d-1)}{2} = \frac{fb}{2\tau}(\frac{1}{d-1} - \frac{1}{d+1}) \tag{5}$$

Clearly, a system with better depth resolution will be able to estimate velocity faster and more accurately.

Vehicle braking performance Latency and inertia in the braking system must be considered. First, the driver takes time, t_d, to respond to a warning and push the brake pedal [13]. Second, our vehicle slows down to V^i_{crit} in

$$t_b = \frac{V^i - V^i_{crit}}{2\mu g} \tag{6}$$

where μ is a coefficient of friction appropriate for the road conditions modelled [14]. Thus, after a warning is issued, our vehicle travels a distance,

$$D_b = V^i t_d + \frac{(V^i)^2 - (V^i_{crit})^2}{2\mu g} \tag{7}$$

while it slows down to V^i_{crit}.

2.5 Measurements at each sample for each feature point

For each feature point $(u_{L|R}, v, d)$ the measured location is

$$\overrightarrow{\widehat{O}^r} = \begin{bmatrix} \widehat{X}^r \\ 0 \\ \widehat{Z}^r \end{bmatrix} = \frac{b}{d} \begin{bmatrix} u \\ 0 \\ f/\tau \end{bmatrix} - \begin{bmatrix} \frac{b}{2} \\ 0 \\ 0 \end{bmatrix} \tag{8}$$

In a safe system, we must consider all measurement errors.
As we show, this is particularly important here because, due to the discrete sensor pixels, disparities are integral and measured Z values lie in a discrete set, separated by disparity change boundaries (shown as horizontal dotted lines in Figure 8). This causes significant errors in trajectory estimates. As shown earlier[9], this error however reduces significantly as the object crosses disparity change boundaries. Discrete pixels introduce an error in X measurements too.
X measurement error arises from discrete pixels also but is magnified by the distance, $\widehat{Z}^r$, to the feature point. So, the actual position for a point observed at u with disparity, d lies in the area bounded by the four points:

$$\overrightarrow{O}_q^r = \begin{bmatrix} \left(Z(d) \pm \left(\frac{Z(d)-Z(d+1)}{2}\right)\right)\left(\frac{\tau}{f}\right)\left(u \mp \frac{\tau}{2}\right) - \frac{b}{2} \\ 0 \\ Z(d) \pm \left(\frac{Z(d)-Z(d+1)}{2}\right) \end{bmatrix} \tag{9}$$

where the four values for $q = \{0, 1, 2, 3\}$ are obtained by taking all combinations of +,- for the $\pm$ and $\mp$ operators: $q = 0 : \pm = +, \mp = +; q = 1 : +, -; q = 2 : -, -; q = 3 : -, +$. Note that $q = 2$ represents the nearest point to our vehicle in the region of uncertainty.

Object velocity estimation We denote the observed position of the j^{th} point in frame, k, as $\overrightarrow{\widehat{O}^r_{q,k,j}}$ (extending the notation of Equation 9).
For frame k, the relative velocity, $\overrightarrow{\widehat{V}^r_j}$, for feature point j, ranges between

$$\overrightarrow{min_j V^r} = \frac{1}{t} \begin{bmatrix} \widehat{X}^r_{2,k,j} - \widehat{X}^r_{0,0,j} \\ 0 \\ \widehat{Z}^r_{3,k,j} - \widehat{Z}^r_{1,0,j} \end{bmatrix} \tag{10}$$

and

$$\overrightarrow{max_j V^r} = \frac{1}{t} \begin{bmatrix} \widehat{X}^r_{1,k,j} - \widehat{X}^r_{0,0,j} \\ 0 \\ \widehat{Z}^r_{1,k,j} - \widehat{Z}^r_{2,0,j} \end{bmatrix} \tag{11}$$

where t is the time between frame k and 0 and $X_{q,k,j}$ is the X component of $\overrightarrow{\widehat{O}^r_q}$ in the k^{th} frame for j^{th} feature point.
After the first change in disparity, the assumption that the object moves at constant velocity allows the velocity extremes to be truncated to the maximum

values consistent with all previous observations. After further changes in disparity, the velocity uncertainty reduces further, but it is probably not wise to continue to assume constant velocity as objects will often change velocity, therefore we only apply this constraint over one disparity change so as to model a more realistic scenario in which some change in object velocity may be expected. Thus the 0 in Eqns 10 and 11 should be replaced by the index of the frame at which the previous disparity change was observed.
Each feature point has its own range of velocities. Since we assume a rigid body, in which all points move at the same velocity, the system chooses the largest minimum and the smallest maximum as the range of velocities consistent with all feature point observations, so for the whole object:

$$\overrightarrow{maxV^r} = \begin{bmatrix} min\left(max_1 V_x^r, max_2 V_x^r, \ldots, max_n V_x^r\right) \\ 0 \\ min\left(max_1 V_z^r, max_2 V_z^r, \ldots, max_n V_z^r\right) \end{bmatrix} \tag{12}$$

$$\overrightarrow{minV^r} = \begin{bmatrix} max\left(min_1 V_x^r, min_2 V_x^r, \ldots, min_n V_x^r\right) \\ 0 \\ max\left(min_1 V_{z,}^r min_2 V_z^r \ldots, min_n V_z^r\right) \end{bmatrix} \tag{13}$$

After each observation, the velocity range reduces, but it never reaches zero. After frame two, the extremes of the velocity range often represent speeds which are unrealistically high for the current traffic scenario, *e.g.* a speed of over $100km/h$ is rare in dense urban traffic. These high possible speeds mean that the system must warn of a possible collision after the second frame when, in fact, one is extremely unlikely. To avoid excessive false warnings, the model assumes that the highest speed of an object cannot be more than a 'speeding factor' (s) times the legal limit: $V_{max} = sV_{limit}$.
The range of trajectory angles, (ρ_L,ρ_R), is then computed from the truncated $\overrightarrow{minV^r}$ and $\overrightarrow{maxV^r}$. Figure 3 shows a typical narrowing of the range of trajectory angles.

Tangent angles After converting the j^{th} feature point's nearest measured position, to polar co-ordinates in (X,Z) plane: $\overrightarrow{\widehat{O}_{2,k,j}^r} \to (D, \zeta)$. The tangents to our vehicle's exclusion zone are:

$$\zeta_L = \zeta - sin^{-1}\left(\frac{r_{exc}}{D}\right) \quad \zeta_R = \zeta + sin^{-1}\left(\frac{r_{exc}}{D}\right) \tag{14}$$

System states The system associates one of the following states with any object observed in the scene:

- **S0** – First frame, only distance is known.
- **S1** – Object will not collide with us.
- **S2** – Object may collide, but safe to make further observations.
- **S3** – Object may collide, but not safe to make further observations – issue precautionary warning.
- **S4** – Object will definitely collide with us – issue necessary warning.

Judging a collision When an object is first observed (frame $k = 0$ for that object), its state is **S0**. After observation $k > 0$, the system computes (ρ_L,ρ_R) for the nearest possible location of the j^{th} feature point, $\overrightarrow{\widehat{O}^r_{2,k,j}}$. If ($\rho_L$,$\rho_R$) includes the collision trajectory, ζ, the system flags a possible collision (states **S2**, **S3** or **S4**), otherwise it is safe (**S1**).
The advantages of considering set of feature points over the extent of object instead of a single reference point are:

- Constraints between the feature points narrow the trajectory range.
- Range of trajectories immediately reduces when a feature point crosses a disparity change boundary.
- Trajectories which are avoiding for one feature point - trajectories outside (ζ_L, ζ_R) - could be colliding - within (ζ_L, ζ_R) - for the other feature points. So, if the extremes of the trajectory range for any feature point intersect the exclusion zone, then the system issues a necessary warning (state **S4**). Otherwise, the system is either at **S2** or **S3**. Algorithm 1 and Algorithm 2 show how our system judges a collision.

The system uses the nearest observed feature points in the $X - (j = jx)$ and $Z - (j = jz)$ directions and checks whether it is safe to consider additional observations (state **S2**) or not (**S3**) (see Algorithm 3). Considering additional observation allows the system to refine the object trajectory range, (ρ_L,ρ_R), which reduces with each observation.
An example of the transitions between states is shown in Figure 3 which shows how the estimated trajectory range narrows with each observation and the maximum speed threshhold is applied in frame 2.

2.6 Tolerable Speed Contour generation

To generate our 'safe speed' contours, we first set the z-component of the object's velocity, $V^r_z = 0$, compute the trajectory for a collision, $\zeta = tan^{-1}(\frac{-O^r_z(0)}{-O^r_x(0)})$ and use it to compute $V^r_x = \left(V_z - V^i_z\right) \tan\zeta$. We then determine if the stereo system would issue a warning in time to avoid a collision by braking alone (see Section 1). If it could, then V_z is increased until warnings cannot be issued in time.

3 Results and Discussion

3.1 Model Input

The model takes as inputs: the object size $L \times H \times W$, the number of feature points on it, n, the initial object closest point, $[X(0), Y(0), Z(0)]^T$, its velocity, $\overrightarrow{V} = [V_x, V_y, V_z]^T$, the stereo configuration parameters - f, b, pixel size, τ_u, sampling time, δs and d_{max} - and our vehicle parameters - r_{exc}, V^i, V^i_{crit}, t_d, the coefficient of friction, μ, and maximum object speed, V_{max}. See Table 1 for typical values.

Algorithm 1 Computing the maximum tolerable speed

maxTolerableSpeed($\overrightarrow{O(0)}, \overrightarrow{V}, \overrightarrow{V^i}, \overrightarrow{V_{max}}, r_{exc}$,
$n, L, H, W, f, b, \tau, d_{max}, \delta s, t_b, t_d, t_p, D_b$) **returns** speed
Initialize $\overrightarrow{O^r} = \overrightarrow{O(0)}$, $\overrightarrow{V^r} = \overrightarrow{V} - \overrightarrow{V^i}$ and tolerable speed, $\overrightarrow{V_{safe}} = \overrightarrow{0}$
$t = 0$
Initialize the set of feature points over the object extent $\left[\overrightarrow{O^r_{0,1}}, \overrightarrow{O^r_{0,2}}, ..., \overrightarrow{O^r_{0,n}}\right]$
$S \leftarrow$ **S0**
for each observation k in $\{0, 1, \ldots\}$ **do**
  for each feature point j in $\{1, 2, \ldots n\}$ **do**
    Update feature point position $\overrightarrow{O^r_{k,j}} = \overrightarrow{O^r_{0,j}} + \overrightarrow{V^r}t$
    if $\overrightarrow{O^r_{k,j}}$ in stereo CFoV (see Section 2.4) **then**
      Determine $\overrightarrow{\widehat{O}^r_{q,k,j}}$
      Determine $\overrightarrow{min_j V^r}$ and $\overrightarrow{max_j V^r}$
    end if
  end for
  Select feature points (jx, jz) at nearest X and Z distances, $\widehat{X}^r_{2,k,jx}$ and $\widehat{Z}^r_{2,k,jz}$
  if $t > 0$ **then**
    Compute $\overrightarrow{minV^r}$ (Equation 13) and $\overrightarrow{maxV^r}$ (Equation 12) and apply threshold $\overrightarrow{V_{max}}$
    Compute (ρ_L,ρ_R) - trajectory angle range
    Compute tangent angle arrays ($\underline{\zeta_L}, \underline{\zeta_R}$) for each feature point to the exclusion zone
    $S \leftarrow$ **CollisionDecision**($\rho_L, \rho_R, \underline{\zeta_L}, \underline{\zeta_R}, n$) (see Algorithm 2)
    if $S \in \{$**S2**, **S3**$\}$ **then**
      Compute $\overrightarrow{minV}$ from $\overrightarrow{minV^r}$
      $S \leftarrow$ **canWait**($\widehat{X}^r_{2,k,jx}, \widehat{Z}^r_{2,k,jz}, minV_x, minV_z$,
      $V^i_z, t_b, t_d, \delta s, r_{exc}, D_b$) (see Algorithm 3)
    end if
    if $S \in \{$**S3**, **S4**$\}$ **then**
      Check if vehicle can avoid a collision by braking
      if collision is avoidable **then**
        speed $|\overrightarrow{V^r}|$ is safe, set $\overrightarrow{V_{safe}} = \overrightarrow{V}$
      else
        Collision detected, but too late
        return (previous) $|\overrightarrow{V_{safe}}|$
      end if
    end if
  end if
  Consider another observation $t = t + \delta s$
end for

Algorithm 2 Definite or possible collision decision – see Section 2.5

```
CollisionDecision(ρ_L, ρ_R, ζ_L, ζ_R, n) returns system state
Initialize state, S ← S0
for each feature point j in {1, 2, ... n} do
  if no trajectories collide - (ρ_L > ζ_{R,j} OR ρ_R < ζ_{L,j}) then
    Consider next feature point
  else
    if (ρ_L ≥ ζ_{L,j} AND ρ_R ≤ ζ_{R,j}) then
      return S4 (definite collision)
    else
      Set S ← S2
      Compute the overlap (ϱ_{L,j}, ϱ_{R,j}) between (ρ_L, ρ_R) and ζ_{L,j}, ζ_{R,j}
    end if
  end if
end for
if S=S2 then
  Compute the minimum angle ϱ_L and ϱ_R from arrays ϱ_{L,j} and ϱ_{R,j}
  if ϱ_L > ρ_L OR ϱ_R < ρ_R then
    return S2 ⋁ S3
  else
    Sort ϱ_{L,j} and the corresponding ϱ_{R,j} in ascending order with respect to ϱ_{L,j}
    Compute the length l of array ϱ_{L,j}
    Initialize m = 1
    while ϱ_{R,m} ≥ ϱ_{L,(m+1)} AND m < l do
      All angles between ϱ_{L,(m+1)} and ϱ_{R,m} are colliding
      m = m + 1
    end while
    if all trajectories are avoiding with m = 1 then
      return S1
    end if
    if all trajectories are colliding with m = l − 1 then
      return S4
    else
      return S2
    end if
  end if
end if
return S
```

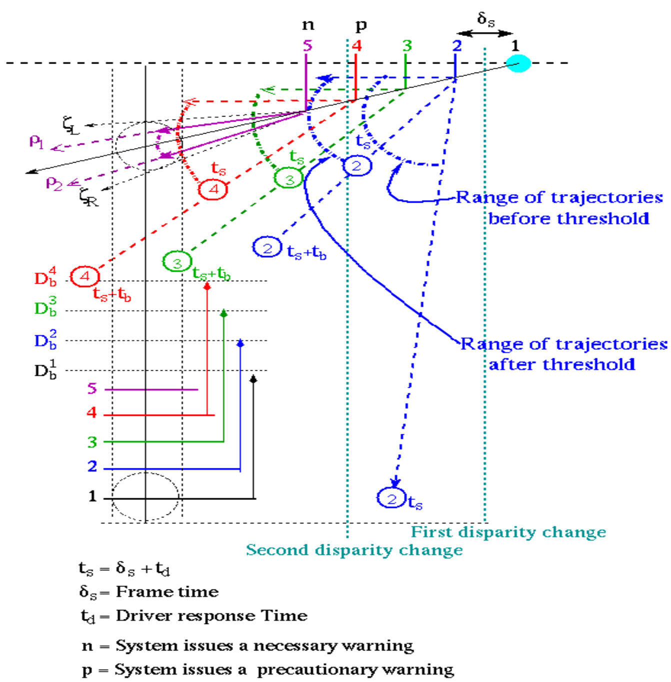

Fig. 3. Paths of object - represented by the nearest feature point on the object - and our vehicle in world co-ordinates. The range of possible trajectories is shown after each observation. Affect of threshold of speeds is shown for observation 2. After observation 4, the system is at state **S3** as it issues a precautionary warning - where an object could be anywhere within the range of possible trajectories but as its worse case represents a collision. While after observation 5 the system could be at state **S4** as it would have issued a necessary warning for a definite collision.

Table 1. System parameters used in the model

Symbol	Description	Typical value
f	Focal length	$5mm$
τ	Pixel size	$4.7\mu m$
b	Baseline length	$750mm$
d_{max}	Maximum disparity	127
ϕ	Vergence angle	$0°$
δs	Sampling interval	0.03 s
r_{exc}	Radius of vehicle exclusion zone	$1m$
V^i	Vehicle speed	17 $ms^{-1}(60kmh)$
V^i_{crit}	Maximum collision speed	$2.77ms^{-1}(10kmh)$ [12]
V_{limit}	Maximum speed limit	$17ms^{-1}(60kmh)$
s	Speeding factor	1.5
t_d	Driver response time	0.5 s [11,13]
μ	Coefficient of friction	0.4 [14,15]
t_p	Object detection and classification time	$1.5ms$
$(L \times H \times W)$	Object size	$(3 \times 0 \times 2)m$
n	Number of feature points	9
Derived Values		
V_{max}	Object maximum speed	$25.5ms^{-1}(90kmh)$
$Z_{min}(d_{max})$	Minimum depth in CFoV	$8.4m$
θ	Half angle of stereo field of view	$25.6°$
t_b	Vehicle braking time	1.8 s ([14])
D_b	Maximum safe braking distance	$44.4m$
Glossary		
ρ_L, ρ_R	Range of trajectory angles for an object	
ζ_L, ζ_R	Trajectory angles with (or tangents to) vehicle exclusion zone	

Algorithm 3 Algorithm for precautionary warnings

canWait($\widehat{X}^r_{2,k,jx}, \widehat{Z}^r_{2,k,jz}, minV_x, minV_z, V^i_z, t_b, t_d,$
$\delta s, r_{exc}, D_b$) **returns** state

Determine whether to issue precautionary warning (S3) because its nearest point will collide in less than the braking time plust a sample time, $t_{bs} = t_d + t_b + \delta s$. Object worst case position after braking would be

$$\overrightarrow{wO^r} = \begin{bmatrix} \widehat{X}^r_{2,k,jx} + minV_x t_{bs} \\ 0 \\ \widehat{Z}^r_{2,k,jz} + minV_z t_{bs} - (D_b + V^i_z \delta s) \end{bmatrix}$$

[$c\zeta_L, c\zeta_R$]=computeTangents($\overrightarrow{wO^r}$) (see Section 2.5)
Maximum vehicle Z-distance to reach V^i_{crit}: $Z_{safe} = V^i_z \delta s + D_b - r_{exc} \cos c\zeta_L$
Minimum object Z-distance after t_{bs}: $wO_z = \widehat{Z}^r_{2,k,jz} + minV_z t_{bs}$
if $wO_z <= Z_{safe}$ **then**
  return **S3** to Algorithm 1
else
  return **S2** to Algorithm 1
end if

3.2 Analysis

Depth resolution degrades with distance, so we take more observations to observe a disparity change for an object which is farther from us. The range of trajectories for an object with feature points close to disparity change boundaries narrows faster than that for an object which lies entirely in a disparity region so that all its points have the same disparity value.

As, with the change in observed disparity, the system now knows that the object is approaching us but it would still be uncertain if it is going to collide with us (or safely cross us). After the disparity change the system infers a velocity as the one consistent with all previous observations. An example is shown in Figure 4 using the Table 1 system parameters for a single reference point. The reference point first appears at $[0, 0, 118]^T$ and is moving with a velocity $\overrightarrow{V} = [0, 0, -0.2]^T$. For the first 9 observations it is observed at the same disparity $d = 9$ with its range of velocities $(max\widehat{V}^r_z - min\widehat{V}^r_z)ms^{-1}$ gradually narrowing down. Due to the introduction of new uncertainty around the newly observed disparity after observation 10, the velocity limit exceeds to -71ms^{-1} instead of the perviously estimated velocity -21ms^{-1}. However, since the new estimate is inconsistent with previous observations so instead the system chooses the last consistent velocity limit of -21ms^{-1}.

3.3 Results

The model outputs a 2D contour map representing the maximum on ground tolerable speeds for the stereo configuration and vehicle parameters.

Figures (5 to 13) present some contour maps for a selection of input values: the typical values in Table 1 with two baseline lengths ($b = 750, 1000$mm) and

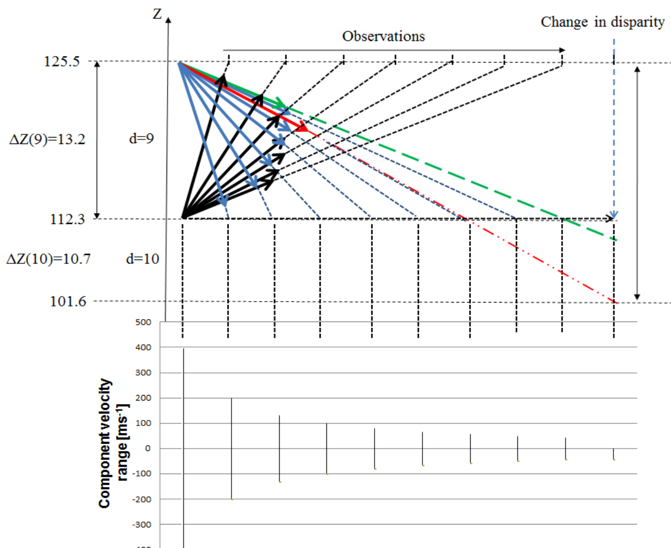

Observation #	0	1	2	3	4	5	6	7	8	9
$\min \hat{V}_z^r$	-	-94	-62	-47	-37	-31	-27	-23	-21	**-21**
$\max \hat{V}_z^r$	-	105	70	52	42	35	30	26	23	**0**
$\max \hat{V}_z^r - \min \hat{V}_z^r$	-	199	132	99	79	66	57	49	44	**21**

Fig. 4. Trajectory Range Narrowing: The range of possible velocities narrows with each observation. Note that once the disparity changes, the lower velocity limit must be consistent with all the previous observations and is shown by the green line (–) - not the red line (–..–) that might be inferred by considering the extreme points (observation 0 and 10) only.

Table 2. Scenarios: Highlights different parameters along with Table 1 configuration parameters used in the discussed scenarios.

Scenario	Object Type	$X(m)$	$Z(m)$	$b(mm)$	$f(mm)$	$V^i_{crit}(kmh)$	$\overrightarrow{V}(ms^{-1})$	$\lvert\overrightarrow{V}\rvert(ms^{-1})$
Sizes	Point($n=1$)	10	144	750	5	10	(-2.9,-25.3)	25.5
	Vehicle($n=9$)	10	144	750	5	10	(-2.9,-25.3)	25.5
V^i_{crit}	Vehicle($n=9$)	10	134	1000	5	10	(-2.9,-25.3)	25.5
	Vehicle($n=9$)	10	134	1000	5	30	(-2.9,-25.3)	25.5
Locations	Point($n=1$)	28	144	750	5	10	(-5.7,-24.8)	25.5
	Point($n=1$)	28	148	750	5	10	(-5.7,-24.8)	25.5

several object sizes (a) point ($n = 1$), (b) pedestrian ($1 \times 1m, n = 9$) and (c) vehicle $(5 \times 2m)$[2].

The tolerable speeds are higher for objects appearing farther away. Note that we have constrained the object speed to $25.5ms^{-1}$(90 kmh in a 60kmh zone).

In the following sections, we have explained in detail how some representative results are derived - first for different sized objects, then different V^i_{crit} for same sized object and finally for different locations. For simplicity, Y components have been omitted from all vectors as we consider motion on the XZ-plane only(see Table 2).

Different sizes First note that, for the chosen scenarios, the braking time is $t_{brake} = t_d + t_b + \delta s = 2.3s$, so that if time to collision is longer than this, we can wait for another observation. We use a typical configuration (*cf.* Table 1) and show how results differ for (a) a single point object ($n = 1$) and (b) a vehicle ($(5 \times 2)m, n = 9$). From Figure 8(a) and (e): both first appear at $(10, 144)m$, moving with $\overrightarrow{V} = [-2.9, -25.3]$ (speed $|\overrightarrow{V}| = 25.5ms^{-1}$). $\overrightarrow{V^r} = [-2.9, -42.3]ms^{-1}$. Table 3 shows the step by step output of the system at each frame. The system uses Algorithm 3 to compute Z_{safe} and wO_z and then determines whether a warning is due (**S3**).

At frame 0, the point is initially observed at $d = 6$. For the vehicle, eight of the nine feature points are initially observed at $d = 6$, while one is observed at $d = 5$. At frame 1, that point has crossed the disparity change boundary from 5 to 6. This change narrows the range of trajectories significantly - the range $(\rho_L - \rho_R)$ goes from (108°—266°) for the point to (180°—266°) for the vehicle. For both objects, at frame 15, a disparity change is observed for the nearest reference point, but the system remains at state **S2**. By frame 19, the single point still has a very wide range of trajectories (180°—267°), whereas the vehicle's range is only (264°—266°). At frame 19, the vehicle's range reduces further to (266.1°—266.8°) and one of the feature points is definitely tracking between our vehicle's exclusion zone tangents (266.1°—266.9°), so the system goes to state **S4** and a warning is issued in time.

For the single point the system does not go to **S3** (causing a warning) until frame 27, but the object is safely avoided. Thus, as the object size increases,

[2] The height of an object is not relevant in the current version of the model - as long as it projects onto at least one image point!

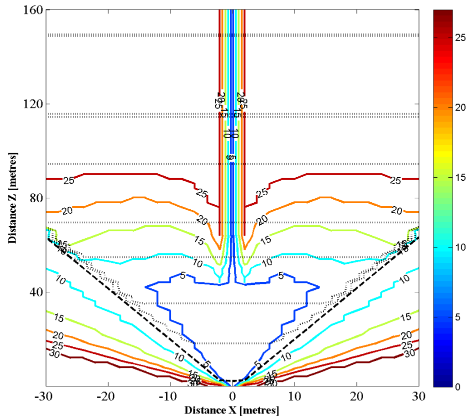

(a) Single point: $b = 750mm$, $f = 5mm$ and $n = 1$

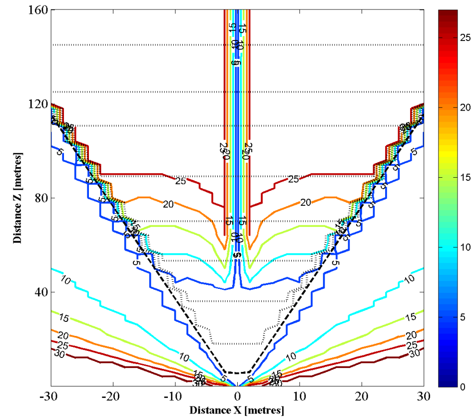

(b) Single point: $b = 750mm$, $f = 9mm$, and $n = 1$

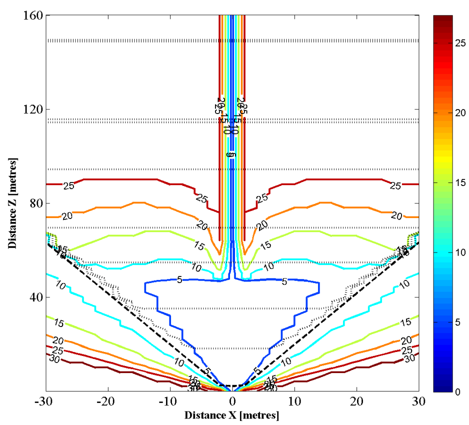

(c) Pedestrian $(1 \times 1)\,m$: $b = 750mm$, $f = 5mm$ and $n = 9$

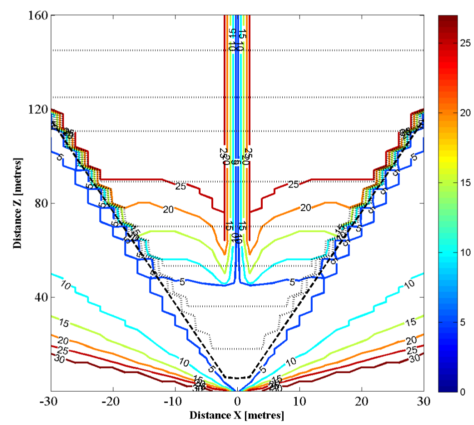

(d) Pedestrian$(1 \times 1)\,m$: $b = 750mm$, $f = 9mm$ and $n = 9$

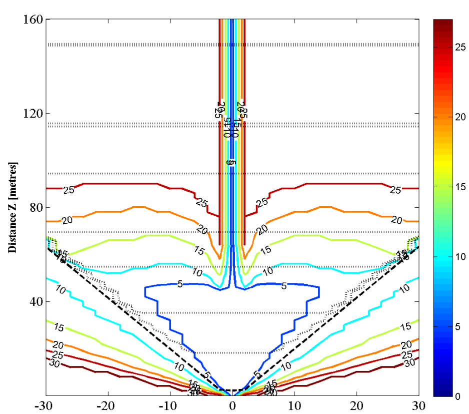

(e) Vehicle $(5 \times 2)\,m$: $b = 750mm$, $f = 5mm$ and $n = 9$

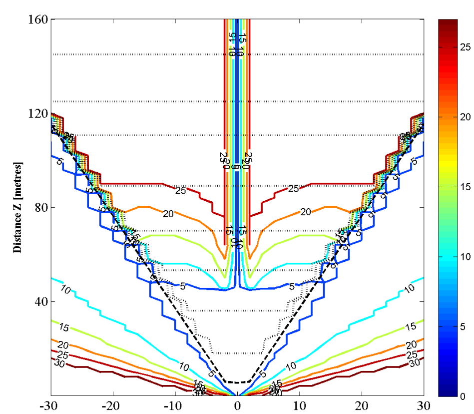

(f) Vehicle $(5 \times 2)\,m$: $b = 750mm$, $f = 9mm$ and $n = 9$

Fig. 5. Tolerable speeds on the ground for various object sizes for Table 1 configuration parameters with $f = (5mm$ or $9mm)$, $b = 750mm$, $(w \times h) = (640 \times 480)$ and $\tau = 7.2\mu m$.

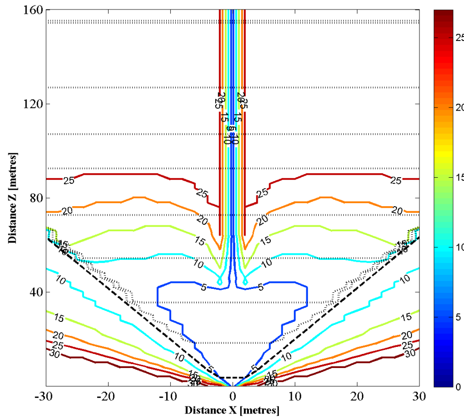

(a) Single point: $b = 1000mm$, $f = 5mm$ and $n = 1$

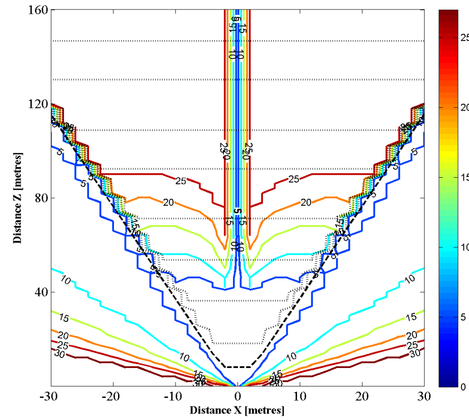

(b) Single point: $b = 1000mm$, $f = 9mm$, and $n = 1$

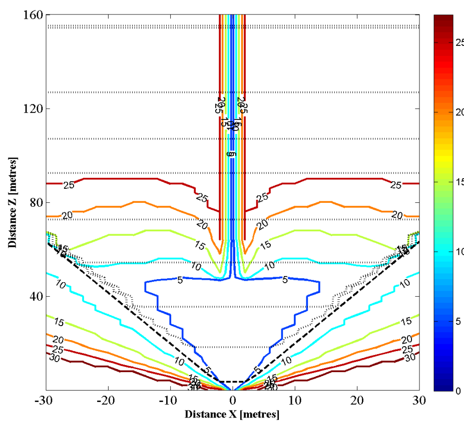

(c) Pedestrian $(1 \times 1)\,m$: $b = 1000mm$, $f = 5mm$ and $n = 9$

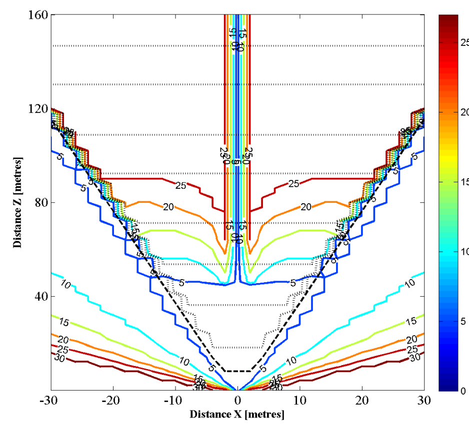

(d) Pedestrian $(1 \times 1)\,m$: $b = 1000mm$, $f = 9mm$ and $n = 9$

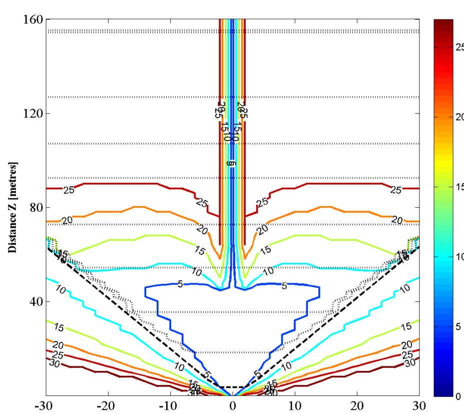

(e) Vehicle $(5 \times 2)\,m$: $b = 1000mm$, $f = 5mm$ and $n = 9$

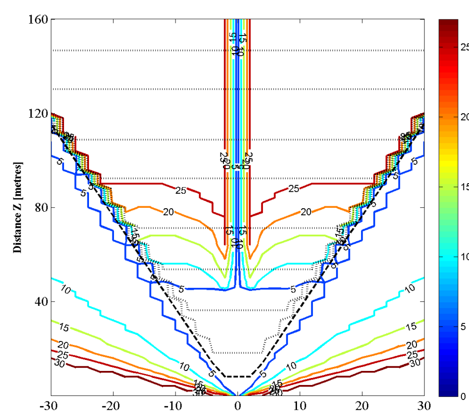

(f) Vehicle $(5 \times 2)\,m$: $b = 1000mm$, $f = 9mm$ and $n = 9$

Fig. 6. Tolerable speeds on the ground for various object sizes for Table 1 configuration parameters with $f = (5mm \text{ or } 9mm)$, $b = 1000mm$, $(w \times h) = (640 \times 480)$ and $\tau = 7.2\mu m$.

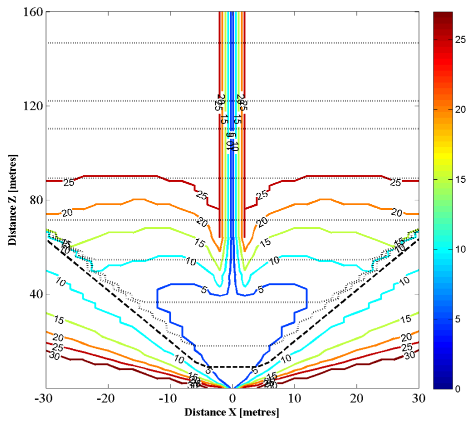

(a) Single point: $b = 2000mm$, $f = 5mm$ and $n = 1$

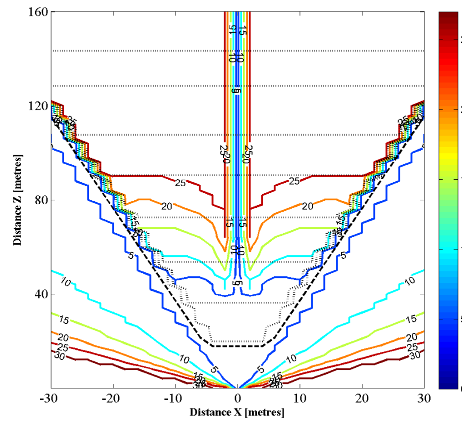

(b) Single point: $b = 2000mm$, $f = 9mm$, and $n = 1$

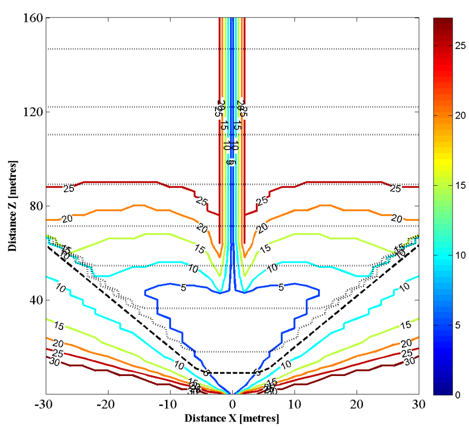

(c) Pedestrian $(1 \times 1)\,m$: $b = 2000mm$, $f = 5mm$ and $n = 9$

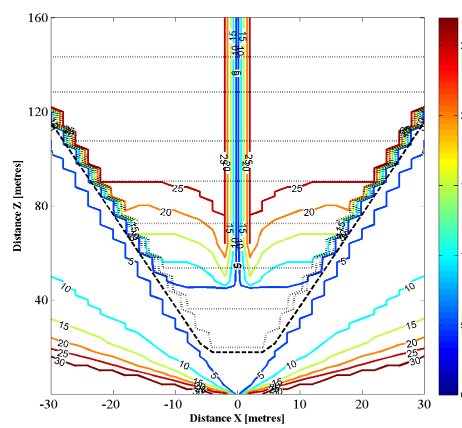

(d) Pedestrian $(1 \times 1)\,m$: $b = 2000mm$, $f = 9mm$ and $n = 9$

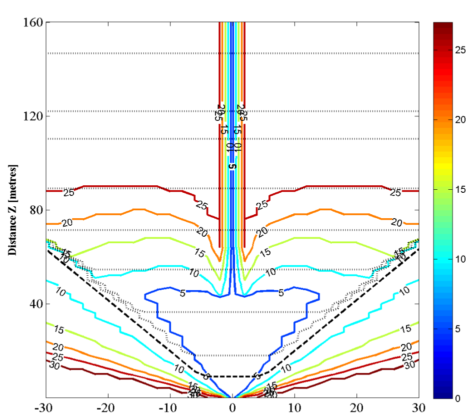

(e) Vehicle $(5 \times 2)\,m$: $b = 2000mm$, $f = 5mm$ and $n = 9$

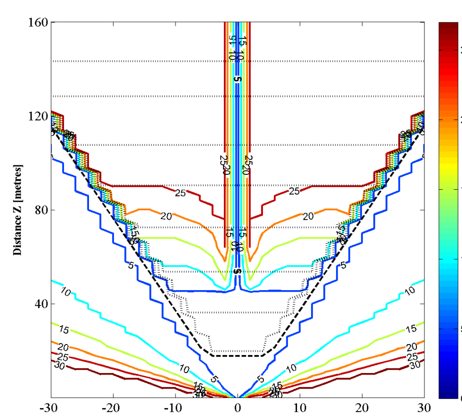

(f) Vehicle $(5 \times 2)\,m$: $b = 2000mm$, $f = 9mm$ and $n = 9$

Fig. 7. Tolerable speeds on the ground for various object sizes for Table 1 configuration parameters with $f = (5mm \text{ or } 9mm)$, $b = 2000mm$, $(w \times h) = (640 \times 480)$ and $\tau = 7.2\mu m$.

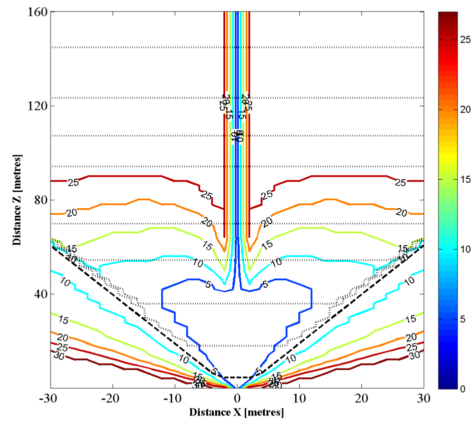

(a) Single point: $b = 750mm$, $f = 5mm$ and $n = 1$

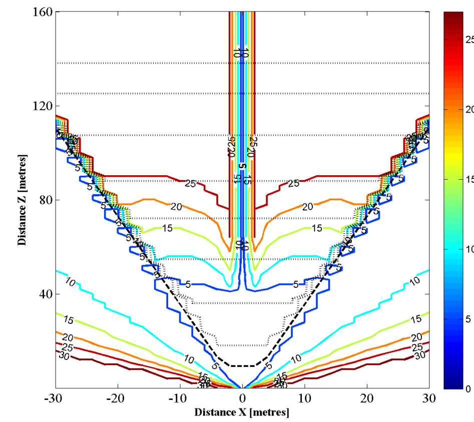

(b) Single point: $b = 750mm$, $f = 9mm$, and $n = 1$

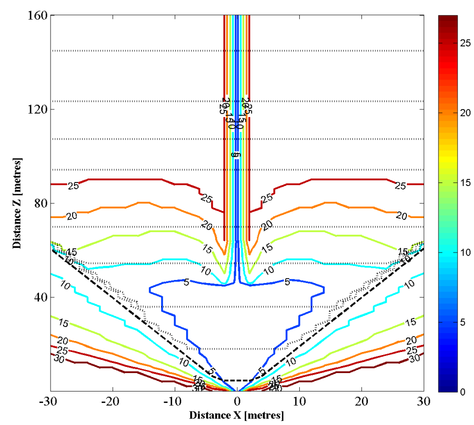

(c) Pedestrian $(1 \times 1)\,m$: $b = 750mm$, $f = 5mm$ and $n = 9$

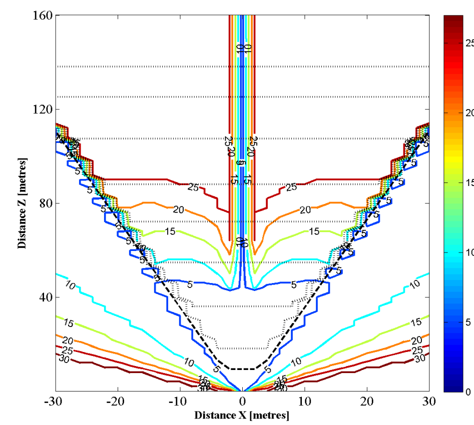

(d) Pedestrian $(1 \times 1)\,m$: $b = 750mm$, $f = 9mm$ and $n = 9$

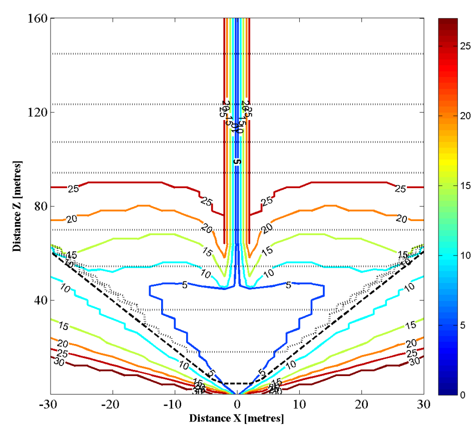

(e) Vehicle $(5 \times 2)\,m$: $b = 750mm$, $f = 5mm$ and $n = 9$

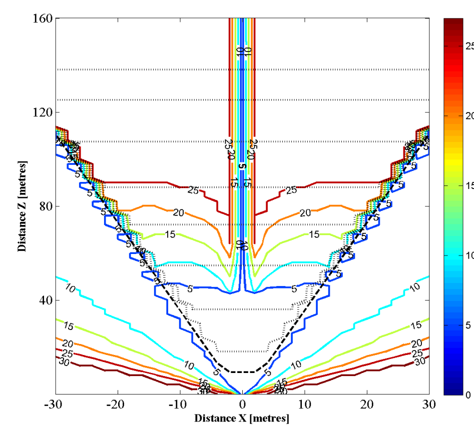

(f) Vehicle $(5 \times 2)\,m$: $b = 750mm$, $f = 9mm$ and $n = 9$

Fig. 8. Tolerable speeds on the ground for various object sizes for Table 1 configuration parameters with $f = (5mm \text{ or } 9mm)$, $b = 750mm$, $(w \times h) = (1024 \times 768)$ and $\tau = 4.7\mu m$.

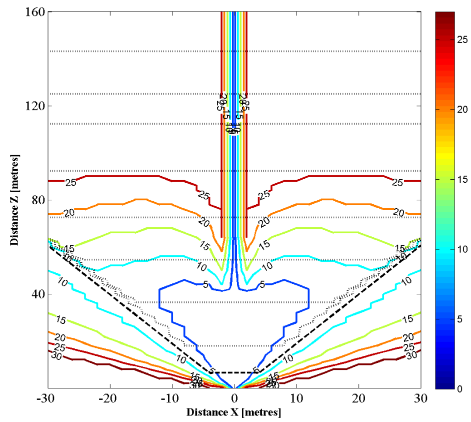

(a) Single point: $b = 1000mm$, $f = 5mm$ and $n = 1$

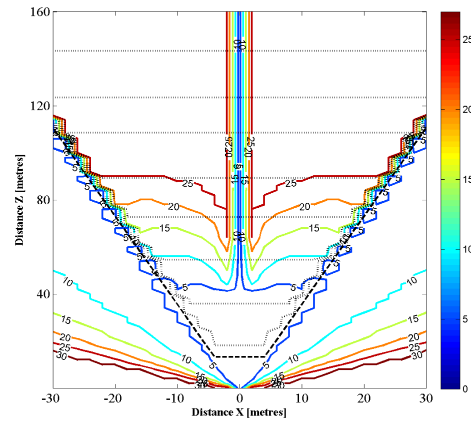

(b) Single point: $b = 1000mm$, $f = 9mm$, and $n = 1$

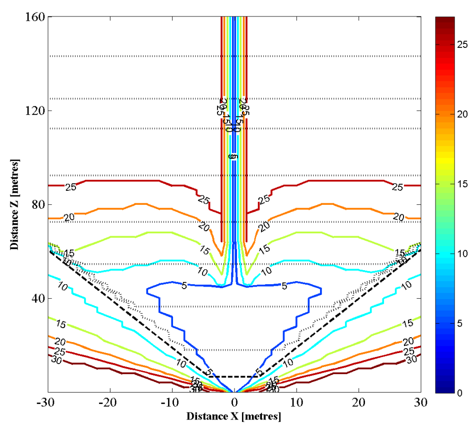

(c) Pedestrian $(1 \times 1)\,m$: $b = 1000mm$, $f = 5mm$ and $n = 9$

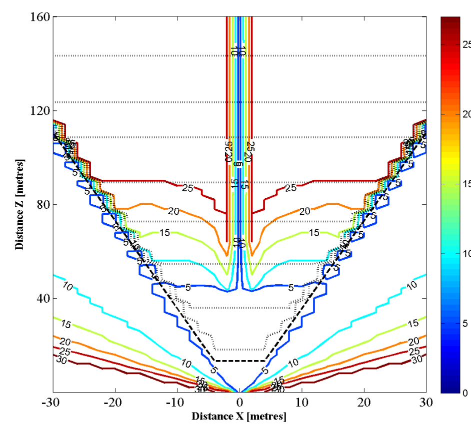

(d) Pedestrian $(1 \times 1)\,m$: $b = 1000mm$, $f = 9mm$ and $n = 9$

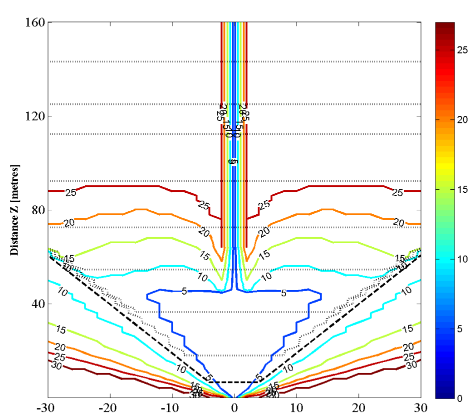

(e) Vehicle $(5 \times 2)\,m$: $b = 1000mm$, $f = 5mm$ and $n = 9$

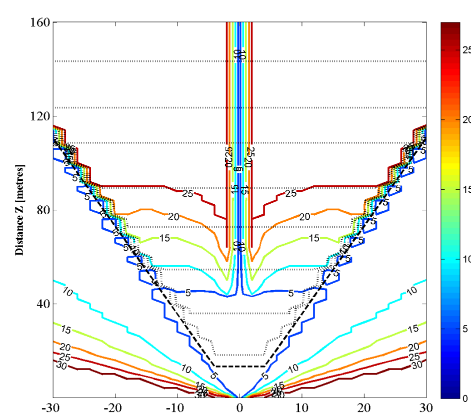

(f) Vehicle $(5 \times 2)\,m$: $b = 1000mm$, $f = 9mm$ and $n = 9$

Fig. 9. Tolerable speeds on the ground for various object sizes for Table 1 configuration parameters with $f = (5mm \text{ or } 9mm)$, $b = 1000mm$, $(w \times h) = (1024 \times 768)$ and $\tau = 4.7\mu m$.

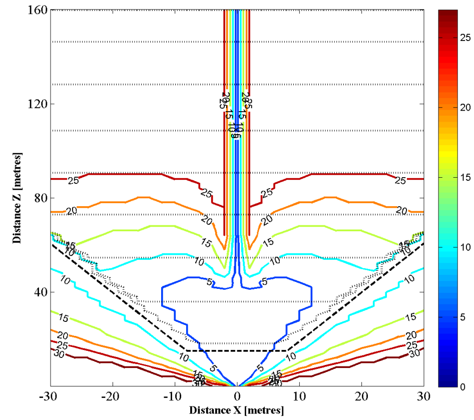

(a) Single point: $b = 2000mm$, $f = 5mm$ and $n = 1$

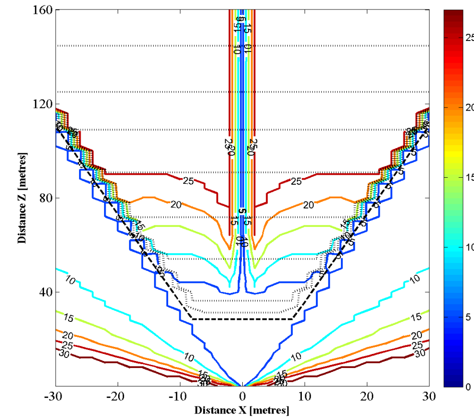

(b) Single point: $b = 2000mm$, $f = 9mm$, and $n = 1$

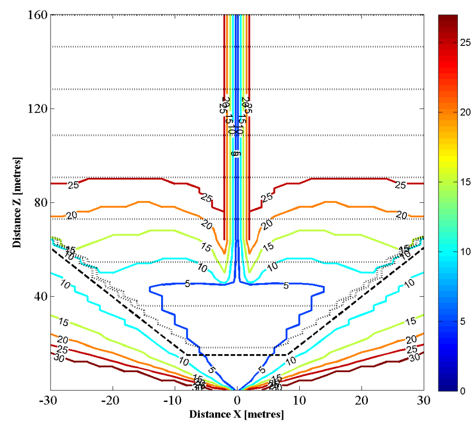

(c) Pedestrian $(1 \times 1)\,m$: $b = 2000mm$, $f = 5mm$ and $n = 9$

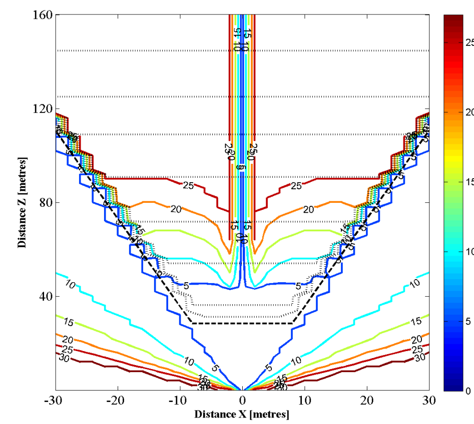

(d) Pedestrian $(1 \times 1)\,m$: $b = 2000mm$, $f = 9mm$ and $n = 9$

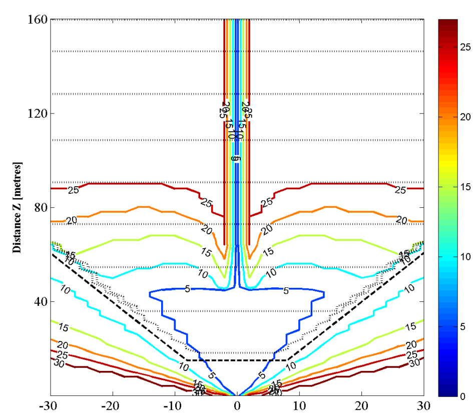

(e) Vehicle $(5 \times 2)\,m$: $b = 2000mm$, $f = 5mm$ and $n = 9$

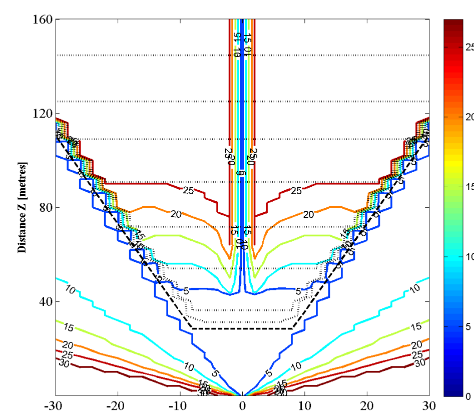

(f) Vehicle $(5 \times 2)\,m$: $b = 2000mm$, $f = 9mm$ and $n = 9$

Fig. 10. Tolerable speeds on the ground for various object sizes for Table 1 configuration parameters with $f = (5mm \text{ or } 9mm)$, $b = 2000mm$, $(w \times h) = (1024 \times 768)$ and $\tau = 4.7\mu m$.

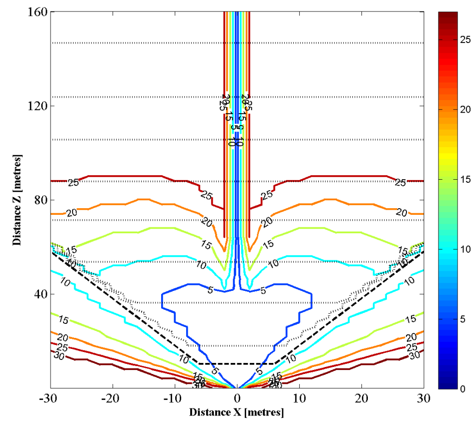

(a) Single point: $b = 750mm$, $f = 5mm$ and $n = 1$

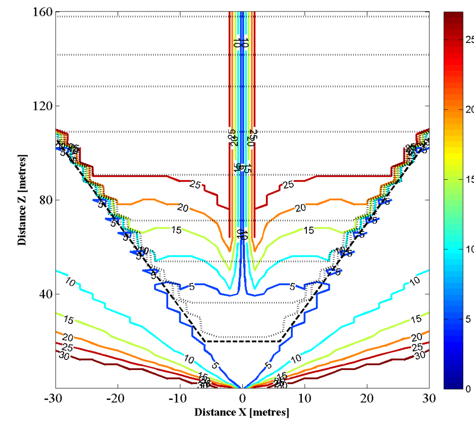

(b) Single point: $b = 750mm$, $f = 9mm$, and $n = 1$

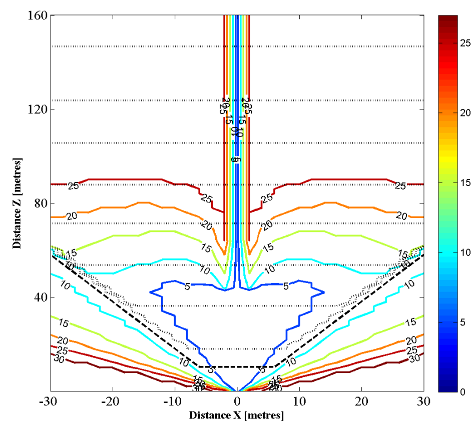

(c) Pedestrian $(1 \times 1)\,m$: $b = 750mm$, $f = 5mm$ and $n = 9$

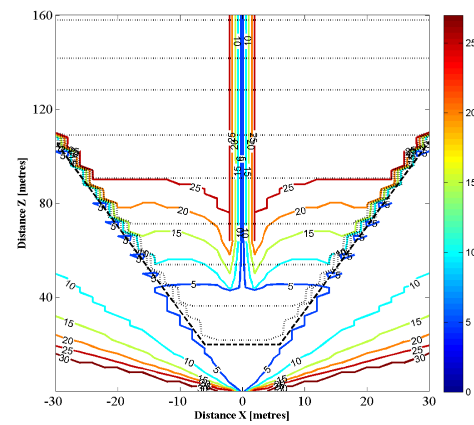

(d) Pedestrian $(1 \times 1)\,m$: $b = 750mm$, $f = 9mm$ and $n = 9$

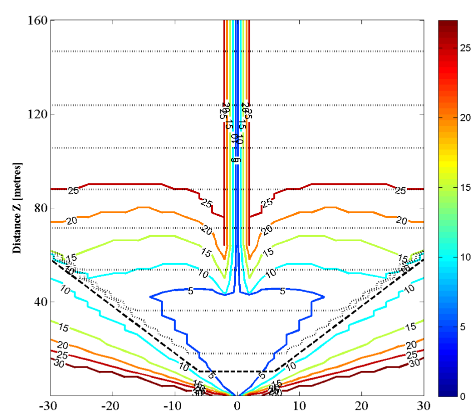

(e) Vehicle $(5 \times 2)\,m$: $b = 750mm$, $f = 5mm$ and $n = 9$

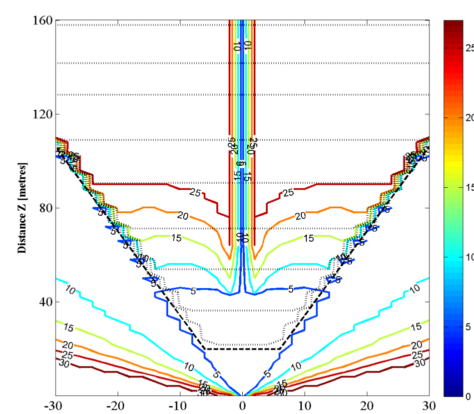

(f) Vehicle $(5 \times 2)\,m$: $b = 750mm$, $f = 9mm$ and $n = 9$

Fig. 11. Tolerable speeds on the ground for various object sizes for Table 1 configuration parameters with $f = (5mm \text{ or } 9mm)$, $b = 750mm$, $(w \times h) = (2048 \times 1152)$ and $\tau = 2.4\mu m$.

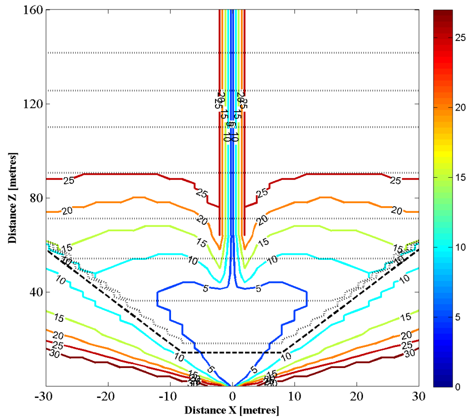

(a) Single point: $b = 1000mm$, $f = 5mm$ and $n = 1$

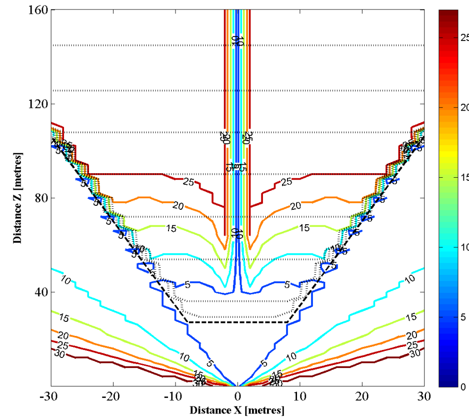

(b) Single point: $b = 1000mm$, $f = 9mm$, and $n = 1$

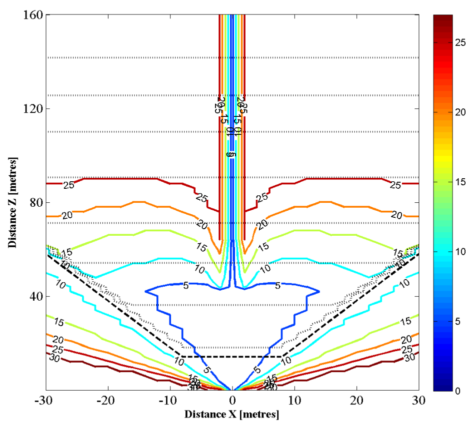

(c) Pedestrian $(1 \times 1)\,m$: $b = 1000mm$, $f = 5mm$ and $n = 9$

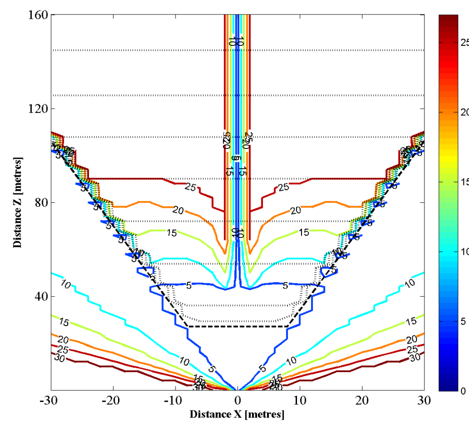

(d) Pedestrian $(1 \times 1)\,m$: $b = 1000mm$, $f = 9mm$ and $n = 9$

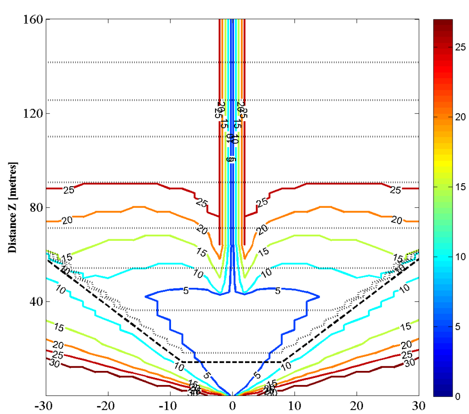

(e) Vehicle $(5 \times 2)\,m$: $b = 1000mm$, $f = 5mm$ and $n = 9$

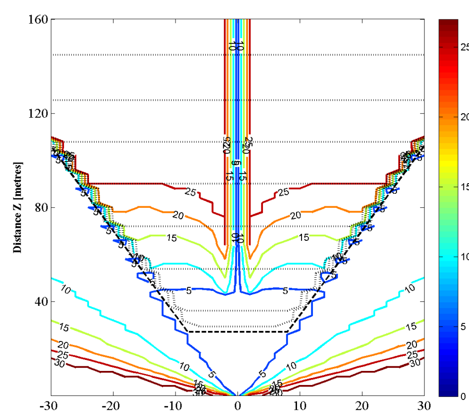

(f) Vehicle $(5 \times 2)\,m$: $b = 1000mm$, $f = 9mm$ and $n = 9$

Fig. 12. Tolerable speeds on the ground for various object sizes for Table 1 configuration parameters with $f = (5mm \text{ or } 9mm)$, $b = 1000mm$, $(w \times h) = (2048 \times 1152)$ and $\tau = 2.4\mu m$.

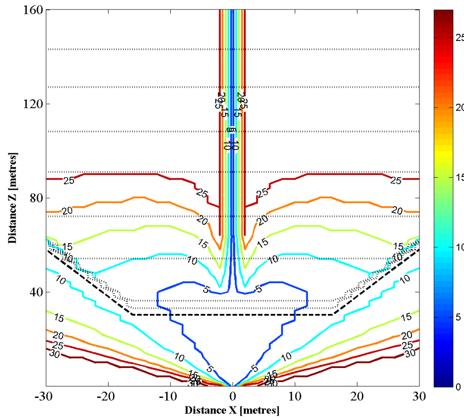

(a) Single point: $b = 2000mm$, $f = 5mm$ and $n = 1$

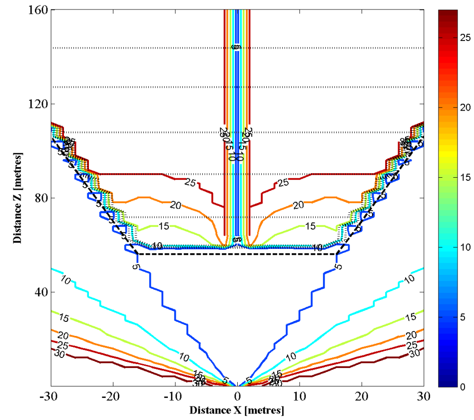

(b) Single point: $b = 2000mm$, $f = 9mm$, and $n = 1$

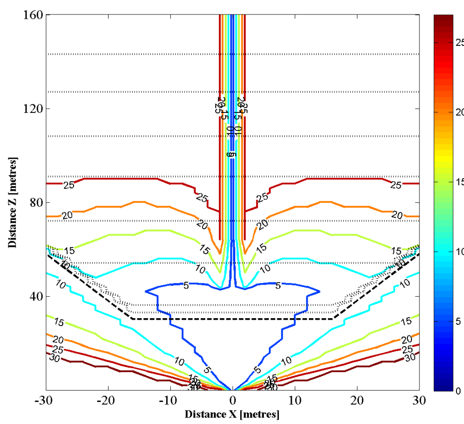

(c) Pedestrian $(1 \times 1)\,m$: $b = 2000mm$, $f = 5mm$ and $n = 9$

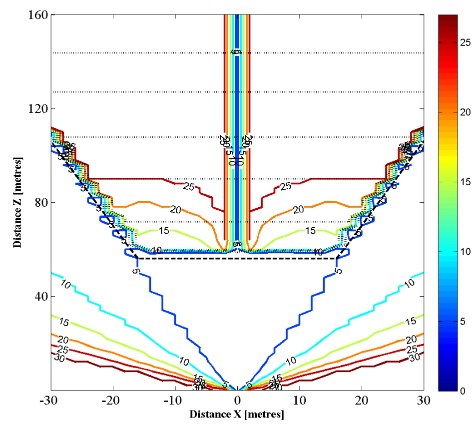

(d) Pedestrian $(1 \times 1)\,m$: $b = 2000mm$, $f = 9mm$ and $n = 9$

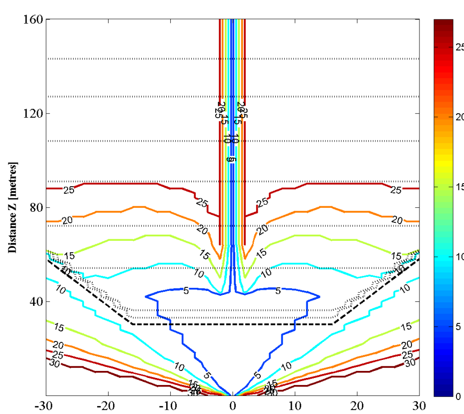

(e) Vehicle $(5 \times 2)\,m$: $b = 2000mm$, $f = 5mm$ and $n = 9$

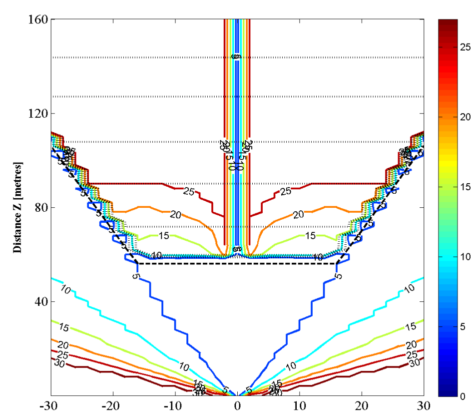

(f) Vehicle $(5 \times 2)\,m$: $b = 2000mm$, $f = 9mm$ and $n = 9$

Fig. 13. Tolerable speeds on the ground for various object sizes for Table 1 configuration parameters with $f = (5mm$ or $9mm)$, $b = 2000mm$, $(w \times h) = (2048 \times 1152)$ and $\tau = 2.4\mu m$.

warnings at state **S4** are issued earlier. For small objects, the system can also issue a timely warning at state **S3** - providing its speed is not higher than the tolerable speed shown in the contour map (Figure 8).

Different V^i_{crit} We use a typical configuration (Table 1) with $b = 1000mm$ and show how the type of warnings differs for a colliding vehicle for (a) $V^i_{crit} = 10kmh = 2.8ms^{-1}$, and (b) $V^i_{crit} = 30kmh = 8.3ms^{-1}$. The colliding vehicle first appears at $(10, 134)m$ moving with $\overrightarrow{V} = [-2.9, -25.3]^T$ (speed $|\overrightarrow{V}| = 25.5ms^{-1}$), $\overrightarrow{V^r} = [-2.9, -42.3]ms^{-1}$(Table 4).
For $V^i_{crit} = 10kmh$, $D_b = 44.4m$ and $t_b = 1.8s$, whereas for $V^i_{crit} = 30kmh$, $D_b = 36.5m$ and $t_b = 1.1s$.
From the frame 0 to 6, the object is observed at $d = 8$. At frame 7, the first disparity change is observed but the range of trajectories is still very wide (180°—267°).
At frame 16, a second disparity change is observed which reduces the possible trajectories to (264°—266°), but its still wider than the tangents to our vehicle's exclusion zone (265°—266°). For $V^i_{crit} = 10kmh$, t_{brake} is longer, therefore the predicted worst case Z-position is $42.4m$ compared to $60m$ for $V^i_{crit} = 30kmh$. So, for $V^i_{crit} = 10kmh$, the system goes to state **S3** and collision is avoided in time.
At frame 19, for $V^i_{crit} = 30kmh$ the system goes to state **S4** as the range of trajectories (265.2°—265.8°) is definitely tracking between the exclusion zone tangents (265°—266°) and the object is safely avoided in time.

Different locations For our typical configuration and a colliding point object ($n = 1$), we show how truncation of the maximum velocity to some 'reasonable' limit (V_{max}) causes the tolerable speed to be the same even though one is farther away.
Consider **P**=$(28, 144)m$ and **Q**=$(28, 148)m$ (see Figure 7(a)). $\overrightarrow{V} = [-5.7, -24.8]$ (speed $|\overrightarrow{V}| = 25.5ms^{-1}$) is tolerable for both. At frame 0, **P** is first observed at $d = 6$ while **Q** is observed at $d = 5$. By frame 2, **P** has moved to $(19.6, 142.6)m$ and is still observed at $d = 6$ because it is still within the limits for $d = 6$ - $123.1m$ to $145.4m$.
At frame 2, **Q** has reached $(19.6, 145.2)m$ and is observed at $d = 6$ having crossed the disparity change boundary at $Z = 145.4m$. However, even after the first disparity change the range of trajectories is still very wide for both and the system considers further observations (state **S2**).
At frame 27, both trajectory ranges are still very wide, but the system can not wait longer so it issues an precautionary warning (state **S3**) for **P** - as the object worst case trajectory would take less than the braking time to collide with us. However, for **Q** the system can still safely consider additional observations (**S2**). At the time of warning **P** is at $(14.8, 106.4)m$ and is safely avoided by braking in time.

At frame 30, **Q** goes to **S3** (precautionary warning). At this time **Q** is at $(14.4, 106.2)m$ and is also safely avoided.

3.4 Warning Types

This stereo based safety system is safe but it issues many unnecessary warnings at state **S3**. Due to the stereo uncertainties the system issues late warnings at state **S4**. Figure 14 shows the tolerable speeds for the Table 1 parameters with $b = 1000mm$ for warnings issued at either: (**S3** or **S4**) or (**S4** only). Note that Figure 14(a) is a copy of Figure 9(e), and is shown again here only for direct comparison.

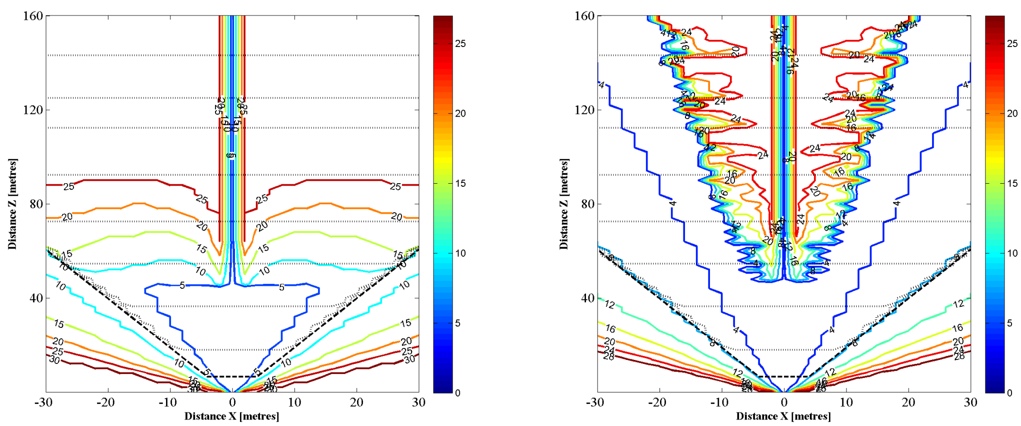

(a) Warnings at states **S3** and **S4**

(b) Warnings at state **S4**

Fig. 14. Difference between tolerable speeds if warnings are only at **S4** compared to the safe situation where the timely warnings are given at (**S3** or **S4**). Colliding object is a vehicle $(5 \times 2)m$ and the system has Table 1 with $b = 1000mm$.

4 Conclusion

The intent of this study was to provide a tool for safety engineer not prescribe stereo configurations as there are many competing constraints (*e.g.* economic, social, *etc.*) beyond the scope of our work. The tool described here enables a designer to assess the effect of competing configuration parameters (*e.g.* $f, b, \tau, w, ..$) against other criteria such as desired opposing object speed. We confine ourselves here to some general observations on the generated maps.

Higher speeds are not tolerated for smaller sized objects, but (luckily!) smaller objects would generally be relatively slowly moving pedestrians. For larger objects, stereo systems can more accurately determine an object's course and issue

an **S4** (definitely needed!) warning. A key factor in the issuing of **S4** warnings (compared to **S3** ones, which are often unnecessary) is observing a disparity change, so the system designer should try to provide high depth resolution in critical regions to increase the probability that disparity changes are observed. As we show, a stereo based safety system can be made 'safe' in the sense that no warnings are missed or late, but may also issue too many warnings due the initial uncertainty in estimation of the opposing object's speed *and* direction. This raises the possibility that simple inexpensive auxiliary devices (*e.g.* SONAR) with limited capabilities (*e.g.* able to locate in one direction only) could be effectively used to reduce the false warnings.
Depth resolution plays an important role in improving tolerable speeds, so verging axis configurations (shown recently to provide better depth resolution[16]) - although they cover significantly different CFoVs - may meet design criteria better and will be investigated next.

References

1. D. Scharstein and R. Szeliski, http://vision.middlebury.edu/stereo.htm.
2. M. Bertozzi, A. Broggi, A. Fascioli, and S. Nichele, "Stereo vision-based vehicle detection," in *IEEE Intell. Vehicles Symposium*, 2000, pp. 39–44.
3. G. N. DeSouza and A. C. Kak, "Vision for mobile robot navigation: A survey," in *IEEE Trans. Pattern Anal. Mach. Intell*, vol. 24, no. 2, 2002, pp. 237–267.
4. Y. Chen, S. Wang, and C. Wang, "Study on vehicle safety distance warning system," in *IEEE Int. Conf. on Industrial Technology*, 2008, pp. 1–6.
5. L. Matthies and S. A. Shafer, "Error modeling in stereo navigation," *IEEE Journal of Robotics and Automation*, vol. 3, no. 3, pp. 239–248, 1987.
6. J. Morris, K. Jawed, and G. Gimel'farb, "Intelligent vision: A first step - real time stereovision," in *Proc. 11th Int. Conf. on Advanced Concepts for Intell. Vision Systems*, ser. LNCS, vol. 5807. Springer, 2009, pp. 355–366.
7. P. Steingrube, S. Gehrig, and U. Franke, "Performance evaluation of stereo algorithms for automotive applications," *Computer Vision Systems*, pp. 285–294, 2009.
8. S. Park and H. Jeong, "A fast and parallel belief computation structure for stereo matching," in *Proc. of the IASTED European Conf.* Anaheim, CA, USA: ACTA Press, 2007, pp. 284–289.
9. W. Khan, J. Morris, and R. Klette, "Stereo accuracy for collision avoidance," in *IVCNZ*, 2009, pp. 67–72.
10. G. Abe and J. Richardson, "The influence of alarm timing on braking response and driver trust in low speed driving," *Safety Science*, vol. 43, no. 9, pp. 639–654, 2005.
11. ——, "The influence of alarm timing on driver response to collision warning systems following system failure," *Behaviour & Information Technology*, vol. 25, no. 5, pp. 443–452, 2006.
12. P. Wramborg, "A new approach to a safe and sustainable road structure and street design for urban areas," in *Proc. Road Safety on Four Continents Conf.*, 2005.
13. R. Dewar, P. Olson, and G. Alexander, *Human factors in traffic safety.* Lawyers & Judges Publishing Company, 2002.

14. A. Tang and A. Yip, "Collision avoidance timing analysis of DSRC-based vehicles." *Accident analysis and prevention*, vol. 42, no. 1, pp. 182–195, 2010.
15. D. Fumi and I. Sultan, "A novel in-vehicle real-time brake-monitoring system," *Proceedings of the Institution of Mechanical Engineers, Part D: Journal of Automobile Engineering*, vol. 223, no. 6, pp. 793–804, 2009.
16. K. Jawed and J. Morris, "Verging axis stereophotogrammetry," in *Pacific-Rim Symposium on Image and Video Technology (PSIVT)*, 2011, pp. 202–213.

Table 3. Point vs. Vehicle: Tolerable speeds of objects first appearing at $[10, 144]^T$ for a point object ($n = 1$) and a vehicle ($(5 \times 2)m, n = 9$) for Table 1 configuration parameters. $Z_{safe} = 45m$.

Point and Vehicle					**Point**		**Vehicle**	
k	**Actual position** $[X, Z]^T m$	d	**Observed position** $(\widehat{X}^r_{2,k,jx}, \widehat{Z}^r_{2,k,jz})$	Object $Z(t_{brake})$ wO_z	**Trajectory range** (ρ_L– ρ_R)	**State**	**Trajectory range** (ρ_L–ρ_R)	**State**
0	(10,144.0)	6	–	–	–	**S0**	–	**S0**
1	(9.9,142.6)		(8.5,123.1)	64	(108°—266°)	**S2**	(180°—266°)	**S2**
2	(9.8,141.2)							
3	(9.7,139.8)							
4	(9.6,138.4)							
5	(9.5,136.9)							
6	(9.4,135.5)				(109°—266°)			
7	(9.3,134.1)				(109°—266°)			
8	(9.2,132.7)							
9	(9.1,131.3)				(110°—266°)			
10	(9.0,129.9)							
11	(8.9,128.5)							
12	(8.8,127.1)							
13	(8.7,125.7)				(112°—266°)			
14	(8.6,124.3)							
15	(8.5,122.8)	7	(7.3,106.7)	47	(180°—266°)		(264°—266°)	
16	(8.4,121.4)							
17	(8.3,120.0)						(265°—266°)	
18	(8.2,118.6)				(180°—267°)			
19	(8.1,117.2)						(266°—266.2°)	**S4**
20	(8.0,115.8)							
21	(7.9,114.4)							
22	(7.8,113.0)							
23	(7.7,111.6)							
24	(7.7,110.2)							
25	(7.6,108.8)				(180°—268°)			
26	(7.5,107.3)							
27	(7.4,105.9)	8	(6.4,94.1)	35	(265.5°—266°)	**S3**		

Table 4. $V^i_{crit} = 10kmh$ and $30kmh$: Tolerable speeds of a colliding vehicle first appearing at $[10, 134]^T$ for Table 1 configuration parameters with $b = 1000mm$. For $V^i_{crit} = 10kmh$ $Z_{safe} = 45m$ and for $V^i_{crit} = 30kmh$ $Z_{safe} = 37m$.

$V^i_{crit} = 10kmh$ **and** $30kmh$					$V^i_{crit} = 10kmh$		$V^i_{crit} = 30kmh$	
k	**Actual Position** $[X, Z]^T m$	d	**Observed position** $(\widehat{X}^r_{2,k,jx}, \widehat{Z}^r_{2,k,jx})$	**Trajectory range** $(\rho_L – \rho_R)$	**Object** $Z(t_{brake})$ wO_z	**State**	**Object** $Z(t_{brake})$ wO_z	**State**
0	(10,134.0)	8	–	–	–	**S0**	–	**S0**
1	(9.9,132.6)		(8.9,125.5)	(108°—266°)	66	**S2**	84	**S2**
2	(9.8,131.2)							
3	(9.7,129.8)							
4	(9.6,128.4)							
5	(9.5,126.9)			(108°—267°)				
6	(9.4,125.5)							
7	(9.3,124.1)	9	(8.1,112.3)	(180°—267°)	53		71	
8	(9.2,122.7)		(7.9,112.3)					
9	(9.1,121.3)							
10	(8.9,119.9)							
11	(8.8,118.5)			(180°—268°)				
12	(8.7,117.1)							
13	(8.6,115.7)							
14	(8.5,114.3)							
15	(8.4,112.9)							
16	(8.3,111.4)	10	(7.4,101.6)	(264°—266°)	42	**S3**	60	
17	(8.2,110.0)		(7.1,101.6)	(265°—266°)				
18	(8.1,108.6)							
19	(8.0,107.2)			(265.2°—265.8°)				**S4**